  Bull. Chem. Soc. Jpn., 61, 1109—1113 (1988)

Dielectric Loss of Dehydrated Rb_3Na_8-ZK4 Zeolite

Tatsuo OHGUSHI
Department of Materials Science, Toyohashi University of Technology, Toyohashi 440
(Received October 12, 1987)

The dielectric properties of completely dehydrated Rb_3Na_8-ZK4 zeolite were studied in the range 12—2.2×10^6 Hz and 211—705 K. Two kinds of losses, relaxation and conduction, were observed. The relaxation loss in the higher-frequency region had an activation energy of 99±2 kJ mol^{-1} and was tentatively assigned to a jump of the Rb^+ ion from an 8-ring site to a vacant 4-ring site. The loss at the lower-frequency region had an activation energy of 95±3 kJ mol^{-1} and was attributed to a movement of the Rb^+ ion on the 8-ring site beyond the unit-cell dimension.

In a recent study on the ^{18}O-exchange between CO_2 and zeolite A, it was confirmed that exchangeable cations migrate out from their normal sites and take part in the formation of an activated complex.[1] Movements of exchangeable cations in a zeolite play a decisive role in the thermal deterioration of its crystallinity and may also play an important role in catalytic processes at higher temperatures. Dielectric measurements are most appropriate for studying cation movement in zeolites, since the jump of cation produces a dielectric loss peak.

Dielectric studies of hydrated zeolites have been carried out by many workers, and various properties have been elucidated. Water in a zeolite increases its electrical conductivity.[2-5] The activation energy in a dielectric relaxation process is seriously influenced by adsorbed water.[3,6-9] However, as pointed out by Jonscher et al.,[10] the dielectric properties of completely dehydrated zeolites have been little known and, thus, the dielectric effect of cationic movements in the completely dehydrated zeolites have not been well understood.

Zeolite A is a leading zeolite for studying the physical and chemical properties of zeolites, and its nature is well-understood. In zeolite A, there exist three structurally distinct cations: those located on the sites of 8-, 6-, and 4-membered oxygen rings, respectively. These cations are abbreviated as an 8-, 6-, and 4-ring cation, respectively, in the following. The distribution of these cations had been studied in detail.[11-20] The presence of three structurally distinct cations makes it too complicate to determine which cation is responsible for a dielectric loss. On the other hand, zeolite ZK4 is isostructural with zeolite A and has two structurally distinct cations, 8- and 6-ring cations,[21] and is appropriate for determining to which cation an observed dielectric loss is to be assigned.

Experimental

Apparatus. The measurement system is shown in Fig. 1. In order to ensure a clean vacuum, parts for an ultrahigh vacuum and a turbo molecular pump were used. Methane is usually evolved, even though in small amounts, from the stainless-steel wall; therefore oxygen was continuously flowed into the system at a pressure level of 5×10^{-4} Pa in order to oxidize methane. At temperatures lower than 470 K, at which the decomposition of methane may not occure, oxygen was not introduced. At temperatures lower than room temperature, helium gas was introduced as a heat conductor, through a helium leaker of quartz kept above 670 K. Dielectric measurements were made with a Cole-Gross-type bridge.[22] A guard electrode is useful for determining the absolute value of the dielectric constant and to reduce the surface leakage current. In the present work, however, we did not require the absolute value of the dielectric constant but, rather, its frequency and temperature dependence; further, the surface leakage current was minimized by vacuum techniques, so that it was not necessary to use the guard electrode, thus avoiding unnecessary complications in the cell system.

Sample. Zeolite ZK4, supplied by Vaughan,[23] had a composition of $Na_{11.0}(AlO_2)_{11.0}(SiO_2)_{13.0}\cdot nH_2O$ (abbreviated as $Na_{11.0}$-ZK4), and was used as a starting material. The zeolite was ion-exchanged with a 0.2 mol dm^{-3} solution of CH_3COORb; its composition was determined by atomic absorption spectrometry to be $Rb_{3.0}Na_{8.0}$-ZK4. Powdery zeo-

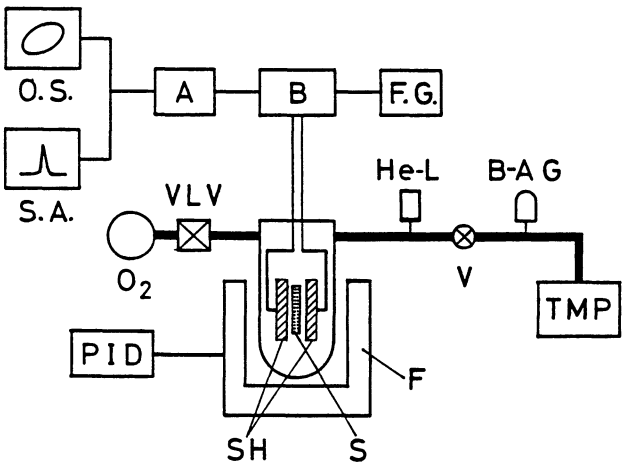

Fig. 1. Apparatus for dielectric measurements.
B: Cole-Gross type brigde, A: amplifier, FG: function generator, OS: oscilloscope, SA: spectrum analyzer, O_2: O_2 gas reservoir, VLV: valiable leak valve, He-L: He leaker, V: stop valve, B-AG, B-A gauge, TMP: turbo molecular pump, PID: PID controller of heater current, SH: sample holder, S: sample, F: electric furnace. Bold line denotes vacuum line.

lite was pressed at a pressure of 900 kg cm^{-2} (8.8×10^7 Pa) at room temperature; the obtained disk had a density of 62% of the single crystal value. The sample did not show any sign of structural damage in its X-ray diffraction pattern and in the water sorption capacity. Thin gold films were evaporated on both sides of the disk for electric contact with gold electrodes. A sample placed in the vacuum system was gently heated under pumping, the temperature being raised by a step of 50 K at an interval of 10 h and finally baked out at 670 K for one day. The back-ground pressure reached was less than 4×10^{-5} Pa. This pressure did not change upon baking out at 670 K for one more day, and was close to the back-ground pressure of the vacuum system without a sample at 670 K, ca. 3×10^{-5} Pa; thus, we judged the sample to be completely dehydrated.

Results

Complex dielectric constants ($\varepsilon^*=\varepsilon'-i\varepsilon''$) were measured as a function of the frequency, f, in the range 12—2.2×10^6 Hz and 211—705 K. Their values measured were not corrected for the packing factor, since we do not need the absolute values (as mentioned above). The sample temperature, T, was controlled, at least, within ±0.5 K of a preset temperature. Data were reproducible in a range of ±1%.

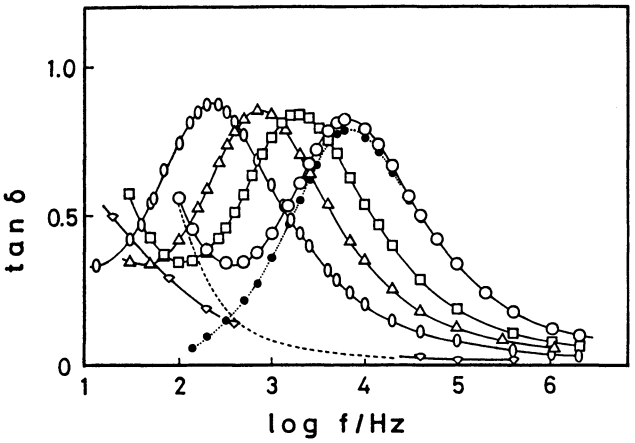

Fig. 2. Spectra of loss tangent. ○: 705.2 K, □: 656.6 K, △: 624.0 K, 0: 588.3 K, ◇: 500.3 K, broken line: loss tangent of conduction ($\tan\delta_c=\varepsilon''_c/\varepsilon'_{obs}$) at 705.2 K, calculated by using relation of $\varepsilon''_c=\sigma/2\pi f\varepsilon_0$ with $\sigma=1.93\times10^{-7}$ S m^{-1}, ●: loss tangent of relaxation ($\tan\delta_r$) at 705.2 K, obtained from relation of $\tan\delta_r=\tan\delta_{obs}-\tan\delta_c$. Subscript obs denotes observed value.

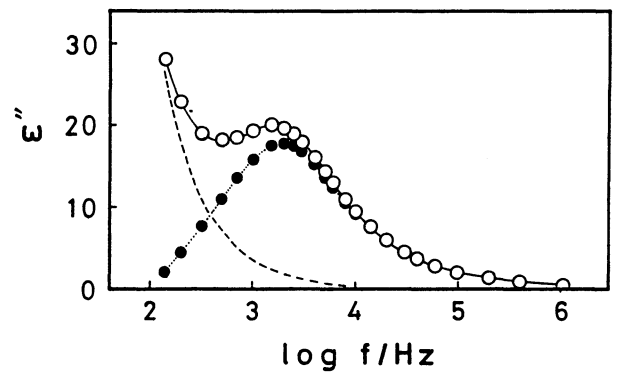

Fig. 3. Spectrum of dielectric loss. ○: observed value at 705.2 K (ε''_{obs}), broken line: conduction loss, ε''_c, calculated from $\varepsilon''_c=\sigma/2\pi f\varepsilon_0$ with $\sigma=1.93\times10^{-7}$ S m^{-1}, ●: relaxation loss ε''_r ($=\varepsilon''_{obs}-\varepsilon''_c$).

The spectra of the loss tangent ($\tan\delta$) and ε'' contain two kinds of losses: one a relaxation loss peak in the higher-frequency region and the other a loss in the lower-frequency region (abbreviated as the low-frequency loss), as shown in Figs. 2 and 3. Let f_{tan} be the applied frequency giving a maximum peak of the loss tangent; we can then approximately determine the activation energy in the relaxation process, E_{tan}, from Arrhenius plots of $\ln f_{tan}$ vs. $1/T$. The value obtained is given in Table 1. In the spectra of ε'' (Fig. 3), the low-frequency loss is described by the conductivity loss expressed as $\varepsilon''_c=\sigma/2\pi f\varepsilon_0$, where σ is the apparent specific d.c. conductivity and ε_0 the permittivity of vacuum. The low-frequency loss gives a steep rise at higher ε' in the Cole-Cole plots (Fig. 4); this rise is a characteristic of the conduction loss.[24] The low-frequency loss has been frequently observed in zeolite systems and is attributed to the conduction loss.[2,7,25,26] Thus, the low-frequency loss in the present system is assigned to the conduction loss. The most appropriate value of σ was determined by the method described in the Appendix; contributions of the conductivity loss and the conductivity loss tangent were calculated as shown in Figs. 2 and 3. From plots of $\ln\sigma$ vs. $1/T$, the activation energy in the conduction process, E_c, was determined, as listed in Table 1. A relaxation loss part, ε''_r, is obtained from the relation

$$\varepsilon''_r=\varepsilon''_{obs}-\varepsilon''_c=\varepsilon''_{obs}-\sigma/2\pi f\varepsilon_0.$$

Cole-Cole plots, ε''_r vs. ε'_{obs}, are well described by a single circular arc, as shown in Fig. 4; this shows that the loss part, ε''_r, contains a single relaxation process. The

Table 1. Activation Energies and Frequency Factor

E_{tan}	$E_{\varepsilon''}$	E_c	log ω_0
99±2	99±2	95±3	11.4±0.2

E: energy in kJ mol^{-1}, ω_0: angular frequency in s^{-1}.

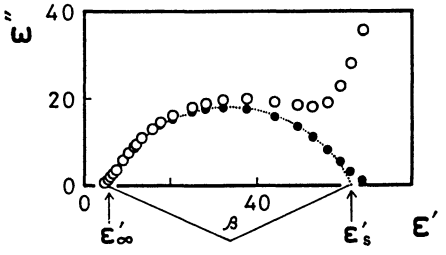

Fig. 4. Cole-Cole plots. ○: observed value at 705.2 K (ε''_{obs} vs. ε'_{obs}), ●: value corrected for conduction loss ($\varepsilon''_{obs}-\varepsilon''_c$ vs. ε'_{obs}, $\varepsilon''_c=\sigma/2\pi f\varepsilon_0$ wth $\sigma=1.93\times10^{-7}$ S m^{-1}) $\varepsilon'_s=61.2$, $\varepsilon'_\infty=5.6$, $\beta=108°$. Subscript obs denotes observed value.

Table 2. Factors of Cole-Cole Circular Arc at Various Temperatures

T/K	ε'_s	ε'_∞	$\varepsilon'_s/\varepsilon'_\infty$	β/deg
705.2	61.2	5.6	11	108
673.9	60.7	5.3	11	109
656.6	61.9	5.6	11	107
624.0	64.0	5.7	11	106
588.3	63.3	5.8	11	102

values of ε'_s, ε'_∞, and β can be determined on the Cole-Cole plots, as shown in Fig. 4 and listed in Table 2, where ε'_s, ε'_∞, and β denote the permittivities at $f\to 0$ and $f\to\infty$, respectively, and the central angle subtended by the circular arc. The frequency, $f_{\varepsilon''}$, giving the maximum value of ε''_r was determined on the spectrum of ε''_r. From Arrhenius plots of $\ln f_{\varepsilon''}$ vs. $1/T$, the activation energy of the relaxation loss, $E_{\varepsilon''}$, and the frequency factor of the jumping cation, ω_o, were obtained as given in Table 1, where ω_o is defined as $\ln f_{\varepsilon''} = \ln \omega_o/2\pi - E_{\varepsilon''}/RT$.

Discussion

The observed values of E_{tan} and $E_{\varepsilon''}$ agree well with each other, as shown in Table 1; this shows that $\varepsilon'_s/\varepsilon'_\infty$ and β are independent of the temperature, since their activation energies are given as[27]

$$E_{tan} = -R\left[\frac{d}{d(1/T)}\ln f_{tan}\right]$$
$$= -R\left[\frac{d}{d(1/T)}\ln f_{\varepsilon''} + \frac{1}{2}\frac{d}{d(1/T)}\frac{1}{\beta}\ln\left(\frac{\varepsilon'_s}{\varepsilon'_\infty}\right)\right]$$

and

$$E_{\varepsilon''} = -R\frac{d}{d(1/T)}\ln f_{\varepsilon''}.$$

As can be seen from Table 2, $\varepsilon'_s/\varepsilon'_\infty$ and β are virtually independent of the temperature. Therefore, one may determine, in the present system, the activation energy of the cation jump in the relaxation process from Arrhenius plots of either $\ln f_{\varepsilon''}$ or $\ln f_{tan}$.

The values of $E_{\varepsilon''}$ and E_c are close to each other. This suggests, as pointed out by Barrer et al.[24] and Rosseinsky et al.,[28] that the relaxation process involves the same cation jump as that in the conduction process. If a charge carrier has a same mechanism in the relaxation process and the conduction process, the dielectric relaxation frequency is related to the specific d.c. conductivity as[29,30]

$$\sigma = \frac{\pi n e^2 d^2 f_{\varepsilon''}}{3kT},$$

where n is the number density of the charge carrier per unit volume, e the elementary charge and d the jump distance. From the equation, one has

$$E_{\varepsilon''} - E_c = RT.$$

In the present experimental conditions, RT is 5—6 kJ mol^{-1} (T is 588—705 K) and the above relation is satisfied within the experimental error.

Let us consider the allowed cation jumps in the zeolite used. There is no data concerning X-ray structural analyses of the Rb_3Na_8-ZK4 zeolite. From X-ray structural analyses of zeolite A, it was found that the Na^+ ion had a stronger affinity for the 6-ring than the Rb^+ ion, and that the Rb^+ ion occupied the center of the 8-ring.[18] It is highly probable that the cations have the same site-affinities in both zeolite A and ZK4. We therefore conclude that $8Na^+$ ions occupy the 6-rings and $3Rb^+$ ions at the centers of the 8-ring in Rb_3Na_8-ZK4 (all 4-ring sites are vacant in zeolite ZK4[21]). A vacant site is necessary for a cation to move. In the above cation distribution, therefore, only three kinds of jumps are allowed. The first is a jump of the Rb^+ ion on the 8-ring to the 4-ring, called Jump I. The 6-ring has two kinds of sites near it, SI and SI', and can accommodate one cation on either site,[16,17] where SI and SI' denote the sites of the large cage side and the sodalite cage side of the 6-ring plane, respectively. The free diameter of the 6-ring is sufficiently large for a Na^+ ion to pass through the ring;[14,15,31] therefore the Na^+ ion can jump between SI and SI', called Jump II. The third is a jump of the Na^+ ion on SI to the 4-ring, called Jump III. In Jumps I—III, only Jump I can contribute to the ionic conduction, since the Rb^+ ion can go away from the unit cell dimension through the route 8-ring→4-ring→another 8-ring. The Na^+ ion has no route to escape from the cell. Consequently, we can assign Jump I to the observed low-frequency loss. This assignment is supported by the results of Haidar et al.[10] They studied the dielectric behaviors of a Ca-A zeolite which was not completely dehydrated, and observed the low-frequency loss. They assigned the loss to a movement beyond the unit-cell dimension of Ca^{2+} ion or ionic species arising from the presence of humidity. In the present zeolite, there is no humidity and, thus, humidity does not become the cause of the low-frequency loss.

If the mechanism of the relaxation loss observed in the present zeolite is same as that of the conduction loss, as suggested above, Jump I is also responsible for the relaxation loss. However, it may be necessary to confirm this assignment by other experiments.

Recently, there has been a discussion concerning the mechanism of the low-frequency loss:[10,32] two kinds, true d.c. and quasi d.c., conduction mechanisms exist. In the present system, measurements could not be made at a sufficiently low frequency range to judge which conduction mechanism was the origin of the low-frequency loss. Whether the low-frequency loss is raised by the true or the quasi d.c. conduction, the charge carrier moves beyond the unit cell dimension and, hence, the assignment of Jump I to the observed low-frequency loss is valid.

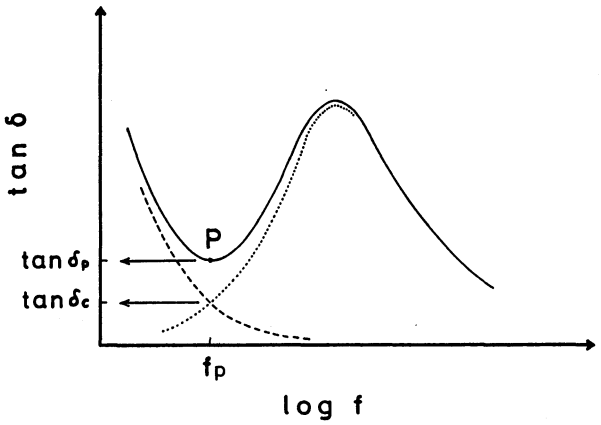

Fig. A-1. Spectrum of loss tangent. Solid line: observed loss tangent, broken line: loss tangent of conduction, dotted line: loss tangent of relaxation, P: saddle point, f_p: frequency at P, $\tan\delta_p$: observed loss tangent at f_p, $\tan\delta_c$: loss tangent of conduction at f_p.

Appendix

In the present system, the low-frequency loss overlaps the relaxation loss. It is desirable to resolve such a composite loss into individual losses in order to study the characteristics of the each loss. The low-frequency loss can be described by $\varepsilon''_c=\sigma/2\pi f\varepsilon_o$. However, there are some arbitrary choices in a determination of the σ-value. Hence, some devices may be necessary in order to determine the σ-value without any arbitrariness. In this Appendix, an approximate determining method is described.

The shape of a loss band and a saddle point clearly manifest themselves in the spectrum of tan δ more than ε''. Hence, the present method can be applied to the spectrum of tan δ. Let tan δ_p and f_p be the values of loss tangent and the frequency at the saddle point P, respectively, as shown in Fig. A-1. At the saddle point, the loss tangent of the conduction, tan δ_c, is approximately equal to the loss tangent of the relaxation, tan δ_r. Then, one has

$$\begin{aligned}\tan\delta_p &= \tan\delta_c + \tan\delta_r \\ &= 2\tan\delta_c. \end{aligned} \quad \text{(A-1)}$$

From the definition of loss tangent, tan δ_p and tan δ_c are written as

$$\tan\delta_p = \frac{\varepsilon''_p}{\varepsilon'_p} \quad \text{(A-2)}$$

and

$$\tan\delta_c = \frac{\varepsilon''_{cp}}{\varepsilon'_p}, \quad \text{(A-3)}$$

where ε'_p and ε''_p denote the observed values of the permittivity and the loss at f_p, respectively, and ε''_{cp} the conduction loss at f_p. The value of ε''_{cp} is expressed as

$$\varepsilon''_{cp} = \frac{\sigma_m}{2\pi f_p \varepsilon_o}, \quad \text{(A-4)}$$

where σ_m denotes the most appropriate value of σ. From the Eqs. A-1—A-4, one obtaines

$$\sigma_m = \pi\varepsilon_o f_p \varepsilon'_p \tan\delta_p$$

or

$$\pi\varepsilon_o f_p \varepsilon''_p.$$

The present author sincerely thanks Prof. Tetsuo Takaishi of Toyohashi University of Technology, for useful discussions, and Dr D. E. W. Vaughan of Exxon Research and Engineerring Co., who supplied ZK4 zeolite. The present work was partially supported by Grant-in-Aid for Encouragement of Young Scientists of the Ministry of Education of the Japanese Government, contract no. 60740232.

References

1) T. Takaishi and A. Endo, *J. Chem. Scoc., Faraday Trans. 1*, **83**, 411 (1987).
2) B. Morris, *J. Phys. Chem. Solids*, **30**, 73 (1969).
3) B. Morris, *J. Phys. Chem. Solids*, **30**, 103 (1969).
4) F. J. Jansen and R. A. Schoonheydt, Reunion Hispano-Berga Miner. Arcilla, An. 1970 (Pub. 1971), p. 45.
5) G. Jones, *J. Chem. Soc., Faraday Trans. 1*, **71**, 2085 (1975).
6) R. M. Barrer and P. J. Coen, *Nature (London)*, **199**, 587 (1963).
7) R. M. Barrer and E. A. Saxon-Napier, *Trans. Faraday Soc.*, **58**, 145 (1962).
8) F. J. Jansen and R. A. Schoonheydt, *Adv. Chem. Ser.*, **121**, 96 (1973).
9) G. Jones and M. Davies, *J. Chem. Soc., Faraday Trans. 1*, **71**, 1791 (1975).
10) A. R. Haidar and A. K. Jonscher, *J. Chem. Soc., Faraday Trans. 1*, **82**, 3535 (1986).
11) T. Takaishi, Y. Yatsurugi, A. Yusa and T. Kuratomi, *J. Chem. Soc., Faraday Trans. 1*, **71**, 97 (1975).
12) A. Yusa, T. Ohgushi, and T. Takaishi, *J. Phys. Chem. Solids*, **38**, 1233 (1977).
13) T. Ohgushi, A. Yusa and T. Takaishi, *J. Chem. Soc., Faraday Trans. 1*, **74**, 613 (1978).
14) J. J. Pluth and J. V. Smith, *J. Am. Chem. Soc.*, **102**, 4704 (1980).
15) V. Subramanian and K. Seff, *J. Phys. Chem.*, **81**, 2249 (1977).
16) J. J. Pluth and J. V. Smith, *J. Phys. Chem.*, **83**, 741 (1979).
17) P. C. W. Leung, K. B. Kunz, K. Seff, and I. E. Maxwell, *J. Phys. Chem.*, **79**, 2157 (1975).
18) R. L. Firror and K. Seff, *J. Am. Chem. Soc.*, **99**, 1112 (1977).
19) T. B. Vance, Jr. and K. Seff, *J. Phys. Chem.*, **79**, 2163 (1975).
20) R. L. Firror and K. Seff, *J. Am. Chem. Soc.*, **99**, 6249 (1977).
21) D. W. Breck, "Zeolite Molecular Sieves," John Wiley & Sons, New York (1974), p. 179.
22) R. H. Cole and P. M. Gross Jr., *Rev. Sci. Instr.*, **20**, 252 (1949).
23) R. H. Jarman, M. T. Melchior and D. E. W. Vaughan, "Intrazeolite Chemistry," ed by G. D. Stucky and F. G. Dwyer, Am. Chem. Soc., Washigton (1983), p 267.

24) R. M. Barrer and E. A. Saxon-Napier, *Trans. Faraday Soc.*, **58**, 156 (1962).
25) F. J. Jansen and R. A. Schoonheydt, *J. Chem. Soc., Faraday Trans. 1*, **69**, 1338 (1973).
26) R. A. Schoonheydt and W. Wild, *J. Chem. Soc., Faraday Trans. 1*, **70**, 2132 (1974).
27) K. S. Cole and R. H. Cole, *J. Chem. Phys.*, **9**, 341 (1941).
28) D. R. Rosseinsky, J. S. Tonge, J. Berthelot, and J. F. Cassidy, *J. Chem. Soc., Faraday Trans. 1*, **83**, 231 (1987).
29) D. R. Rosseinsky, J. A. Stephan, and J. S. Tonge, *J. Chem. Soc., Faraday Trans 1*, **77**, 1719 (1981).
30) S. Bone, J. Eden, P. R. C. Gascoyne, and R. Pething, *J. Chem. Soc., Faraday Trans. 1*, **77**, 1729 (1981).
31) "Handbook of Chemistry and Physics," 66th ed, CRC Press, Boca Raton, Florida (1985), p. F164.
32) A. K. Jonscher and A. R. Haidar, *J. Chem. Soc., Faraday Trans. 1*, **82**, 3553 (1986).